Attenuation of high frequency Signals in Structured Metallization on Glass: Comparing Different Metallization Techniques with 24 GHz, 77 GHz and 100 GHz Structures

Martin Letz[1], Matthias Jost[8], Brandon T. Gore[2], William J. Kozlovsky[2], Romeo Premerlani[3], Alex Bruderer[3], Manuel Martina[4], Thomas Gottwald[4], Tetsuya Onishi[5,6], Shigeo Onitake[6], Siddharth Ravichandran[7], Holger Maune[8], Mathias Mydlak[1]

[1]SCHOTT AG, Hattenbergstr. 10, 55122 Mainz, Germany, [2]Samtec, Colorado Springs, CO 80919 USA , [3]Varioprint AG, Mittelbissaustrasse 9, CH-9410 Heiden, Switzerland, [4]Schweizer Electronic AG, Einsteinstrasse 10, 78713 Schramberg, Germany, [5]Grand Joint Technology Ltd., Hong Kong, [6]KOTO Electric Co., 2-17-3 Ryusen, Taito-Ku, Tokyo 110-0012, Japan, [7]Packaging Research Center, Georgia Tech, 813 Ferst Drive NW, Atlanta, GA 30332, USA, [8]Institute for microwave engineering and photonics, TU Darmstadt, Merckstr. 25, 64283 Darmstadt, Germany
e-mail: Martin.Letz@schott.com

***Abstract*— A number of glass substrates made from the SCHOTT glass AF32_eco in a thickness of 0.1mm are metallized with different processes. On the metallized glass substrates, microstrip lines as well as ring resonator structures are realized which are optimized for frequencies of 24 GHz, 77 GHz and 100 GHz. A careful analysis of the S-parameters of these structures allows to extract the influence of the metallization on the attenuation of microstrip lines as well as quality factors of the resonating structures. The particular metallization process plays a crucial role for the GHz performance and the 'best-of' metallization performs comparable with corresponding structures realized on Rogers RO3003 substrates.**

Keywords: glass substrate, high-Q, glass package, integrated passives, 5G, mobile communication

I. Introduction

The demand for applications at higher GHz frequencies is strongly increasing. It is driven by the race for bandwidth in all types of wireless communication applications which are beginning to fill the frequency range above 6 GHz. It is further driven by applications like automotive radar around 77 GHz or gesture recognition around 60 GHz. Even applications above 100 GHz are more and more discussed in literature. With increased crowding of applications and usage of such frequency bands, the geometric accuracy for all designs and high frequency (HF) structures becomes more crucial.

Glass is a class of materials which is produced with extremely high homogeneity. For example, in standard optical glass production, glasses with dimensions of order of 30 cm are made with refractive index variations which are smaller than $\Delta n/n < 10^{-5}$. Since the dielectric constant is the square of the refractive index $\varepsilon = n^2$, this information is also relevant for electronic applications [1]. Glasses are stiff and show (practically) no plastic deformation under mechanic load and temperature cycling. Glasses have low temperature coefficients of all material properties. In particular they have a thermal expansion which can be adjusted in the range between 0 ppm/K and 12 ppm/K. The higher the frequencies requires that more accurate manufacturing be done. This means that very homogeneous substrates materials with small temperature coefficients and intrinsic stiffness become increasingly important at higher frequency ranges.

In the present study, we choose the glass SCHOTT AF32_eco for a comparative study of different metallization techniques. SCHOTT AF32_eco has a dielectric constant $\varepsilon_r = 5.1$ as well as a dielectric loss at several frequencies of $\tan\delta = 3.5\times10^{-3}$ at 1 GHz, $\tan\delta = 4.9\times10^{-3}$ at 5 GHz, $\tan\delta = 9.0\times10^{-3}$ at 24 GHz and $\tan\delta = 1.1\times10^{-2}$ at 77 GHz. The thermal expansion of the glass is $\alpha = 3.2$ ppm/K, and the temperature coefficient of the dielectric constant at room temperature is $\tau_\varepsilon = 1/\varepsilon \; d\varepsilon/dT = 143$ ppm/K. In Table 1, we show how it compares to other glasses and materials.

In addition to signal transmission lines, resonating and radiating elements as well as integrated passives [5][4][11][12][13] can be integrated in a single advanced package based on glass [9]. Examples for resonating elements are filter elements or L-C network components whereas antenna elements are radiating structures [7]. Even antenna arrays for massive MIMO (multiple in multiple out) antenna arrays with beam steering capability can be realized on a glass substrate. Fields of application for such approaches are e.g. automotive radar at 77 GHz [8] and gesture recognition around 65 GHz.

The higher the frequencies, the more crucial absorption processes, surface roughness and material interfaces become. The dielectric properties of the glass, especially the dielectric loss tangent, $\tan\delta$, can be directly measured, e.g. with resonant spectroscopic methods. The surface roughness of as-drawn glasses from standard hot-forming processes is extremely small. A typical value for a glass like AF32_eco produced in a so called "down-draw" process has a root mean square (rms) value of the roughness of order 0.8 nm. Material interfaces are a more subtle topic and are investigated in the current work. When metallizing glasses adhesion promotors like Ti, Cr, Pd, … which are polyvalent ions and can exist in different oxidation states play a crucial role on the interfaces. Therefore,

the glass-metal interface is one of the largest and unquantified sources of loss in a given structure.

Table 1: Dielectric properties (permittivity ε_r, dielectric loss tanδ and thermal expansion α) of different SCHOTT glasses in comparison with high end RF substrate materials. (*preliminary data, **source data sheet Rogers, *** source data sheet Panasonic, **** source data sheet Isola)

Material	ε_r	tanδ	α / ppm/K
SCHOTT AF32_eco	5.1	4.9×10^{-3} (@5GHz)	3.2
SCHOTT D263T_eco	6.3	10.1×10^{-3} (@5GHz)	7.2
SCHOTT B270D_eco	6.7	7.7×10^{-3} (@5GHz)	9.4
SCHOTT MEMPAX	4.4	7.3×10^{-3} (@5GHz)	3.3
SCHOTT AS87_eco	7.2	17.2×10^{-3} (@5GHz)	8.7
SCHOTT Borofloat33	4.5	7.3×10^{-3} (@5GHz)	3.3
SCHOTT new development	3.9 *	1.7×10^{-3} * (@5GHz)	3.3 *
Rogers RO3003	3.0 **	1.0×10^{-3} ** (@10GHz)	17 (xy-dir.)** 25 (z-dir.) **
Panasonic Megtron 7	3.61 ***	$2.0\ 10^{-3}$ *** (@12GHz)	15 (xy-dir.)*** 42 (z-dir.)***
Isola Astra MT77	3.0 ****	$1.7\ 10^{-3}$ **** (@10GHz)	12(xy-dir.)**** 50 (z-dir.)****

The glasses were metallized and structured at different commercial and academic partners. The metallization consists of copper with a very small layer of adhesive agents and has an overall thickness of at least 6 µm. The differences of these theoretically identical structures are investigated in terms of the metallization quality, propagation and resonating properties. As a reference, all structures were also realized on well-established Rogers RO3003 substrates with a substrate thickness of 0.125 mm.

As a result, the performance of the best metallized samples of SCHOTT glass AF32_eco comes close to the one of the Rogers RO3003 substrate both for the attenuation of the microstrip line (at 24 GHz: 78 dB/m for RO3003 and 83 dB/m for AF32_eco) as well as for the quality factor of the ring resonator (at 24GHz: $Q = 73$ for RO3003 and $Q = 68$ for AF32_eco). This is a surprising result, since the dielectric loss of the PTFE-based substrate in RO3003 ($\varepsilon_r = 3.0$ and tan$\delta = 0.0013$ at 10 GHz) is almost five times lower than for the glass AF32_eco. This proves that this glass is well suited as substrate material for GHz applications but a carefully optimized metallization solution is essential. The reason for the excellent performance of the glass is probably due to the extremely smooth glass surface with rms values smaller than 1 nm as well as the well-defined glass to metal interface. Since glasses can be produced with much smaller dielectric loss if large enough industry demand is present (see e.g. line 7 in Table 1) glass substrates are possible which clearly outperform the electric properties of the best available high end PCB materials like RO3003.

II. Design of Test Structures

The structures were designed to allow (i) contacting of any of the given test structures with standard probe heads from the top side of the substrate. Further, the test structures were (ii) designed with a line impedance of 50 Ω to minimize reflection losses. Also (iii) transmitting structures, microstrip lines of different lengths were designed as well as resonating structures, ring resonators, which showed different weak coupling to the attached microstrip lines.

Contact pads in coplanar waveguide topology were included to the design for RF characterization by means of on-wafer probes. Radial stubs ensure a capacitive coupling of the coplanar waveguide's ground planes to the one of the microstrip line at the back side of the substrate. A microstrip line was chosen since a large part of its electric field is confined in the dielectric substrate, the glass. All designs were conducted using CST Studio Suite. The designs were optimized for 24 GHz, 77 GHz and 100 GHz separately on 0.1 mm thick glass in order to match the line impedance of 50 Ω at the targeted frequency of operation.

Also ring resonators were designed with a resonance close to 24 GHz, 77 GHz and 100 GHz. At 24 GHz, it is designed for the fundamental mode, while for 77 GHz and 100 GHz it is designed for the first and second harmonic, respectively. These ring resonators are weakly coupled to microstrip lines on both sides, separated by small gaps. While the radius of the ring influences the resonance frequency, the width of the gaps between the ring and the microstrip feeding lines are influencing the coupling into the resonator. The smaller the gap, the stronger is the coupling, but at the same time, the loaded quality factor of the resonator is decreasing. Besides that, the quality factor of the resonator contains information on the dielectric loss of the substrate and of the quality of the metallization. A qualitative comparison allows to evaluate and to distinguish between different metallization methods on the same glass substrate.

III. Experimental Setup

Glass Substrate Design

The metallized structures were designed as microstrip lines with different lengths. An example of such a microstrip line with coplanar coupling is shown in Figure 1.

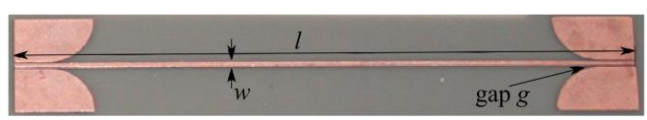

Figure 1: Design of a typical microstrip line with coplanar coupling.

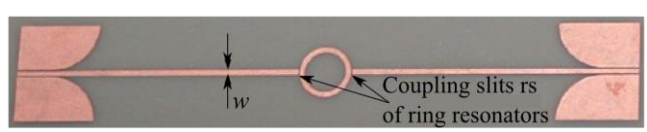

Figure 2: Design of a typical ring resonator with coplanar coupling.

Critical points for this design are the widths of the two gaps in the coplanar waveguide contact pad design and the overall width of the microstrip line. For all structures the width of the copper (Cu) metallization was targeted at $w = 163$ µm to achieve a line impedance of 50 Ω on a 0.1 mm thick AF32_eco glass. For the 24 GHz microstrip lines, the gaps in the coplanar waveguide contact pads were targeted as $g = 76$ µm. The lengths of the structures were chosen to be $l = 37$ mm, 32 mm and 27 mm, respectively. For the 24 GHz ring resonators, the outer diameter of the ring was targeted to be 2.163 mm and the inner diameter 1.837 mm. The gap between the ring and the microstrip line was designed to be rs = 12 µm and rs = 48 µm. For the 77 GHz and 100 GHz structures, the lengths of the microstrip lines was chosen to be 17.1 mm, 12.1 mm and 7.1 mm, respectively. The gap in the coplanar coupling was chosen for both types of structures as 20.3 µm. Also for the ring resonators, the width of the slits between the ring and the microstrip line was targeted for both types of structures as 10 µm and 40 µm. The only difference between the two structures for 77 GHz and 100 GHz is the diameter of the ring resonators. For the 77 GHz structures it was chosen to be 1.373 mm for the outer diameter and 1.0519 mm for the inner diameter to obtain a resonance in the ground mode at 77 GHz. For the 100 GHz structures the diameter of the rings was 1.563 mm outer diameter and 1.241 mm inner diameter to resonate at a second harmonic at 100 GHz.

Measurement procedure

The glass substrate and the substrate of the reference material RO3003 were contacted on a wafer prober from Cascade Microtec with a climate chamber to ensure identical environment for all measurements with respect to temperature and humidity. The contacting for the 24 GHz structures was done using a pair of probe heads with 250 µm pitch (ACP40), see Figure 3. A short-open-load-thru calibration was performed prior to the measurements and the S-parameters were measured using a Keysight PNA-X vector network analyzer (VNA) for the frequencies below 65 GHz and a Keysight PNA combined with two Anritsu 3740A-EW transmission-reflection modules for the frequency range from 65 GHz to 110 GHz. As an example we show the S-parameter S_{11} and S_{12} for three 24 GHz microstrip lines with overall lengths of 27 mm, 32 mm and 37 mm in Figure 4 and Figure 5. In Figure 4 it can be seen that all three lines are well matched to 50 Ω, since the S_{11} parameter circles very close around the center of the Smith chart, the point (1,0). In Figure 5, the three measurements should be parallel lines for ideal measurements where no reflection occurs from impedance mismatch at the contacts. The small reflection is seen in the slight oscillations of the S_{21} measurement. From the difference in the transmission S-parameter S_{12} one can derive the attenuation of the microstrip line in the following way. First the operating power loss

$$T_{\text{eff}} = \frac{|S_{21}|^2}{1-|S_{11}|^2} \quad (1)$$

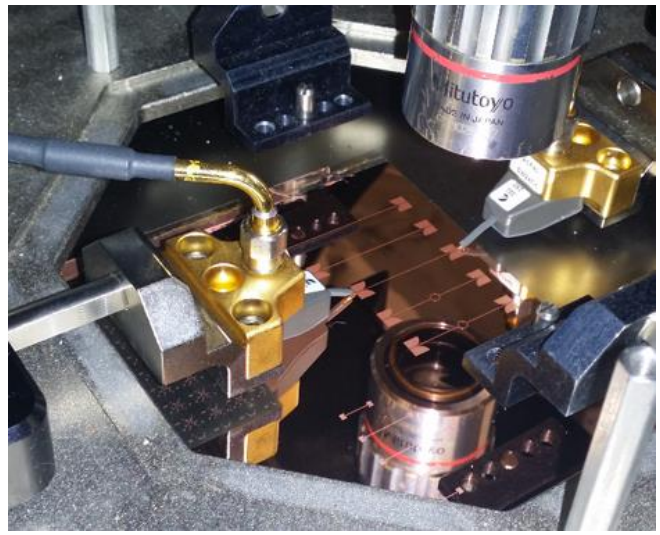

Figure 3: Contacting of the substrate using 250 µm pitch probe heads.

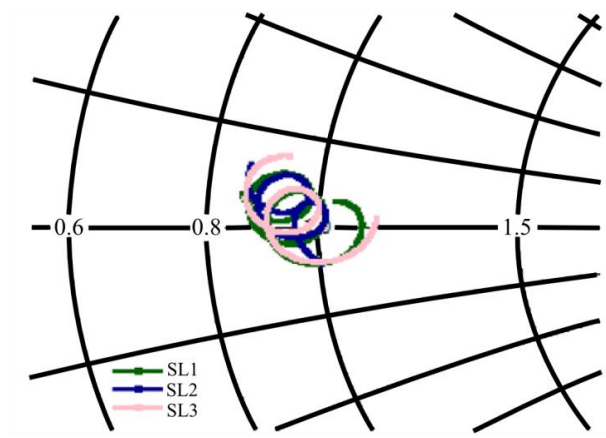

Figure 4: S_{11} parameter plotted in the complex plane (Smith chart) for the three microstrip lines SL1-3 on substrate SM2.

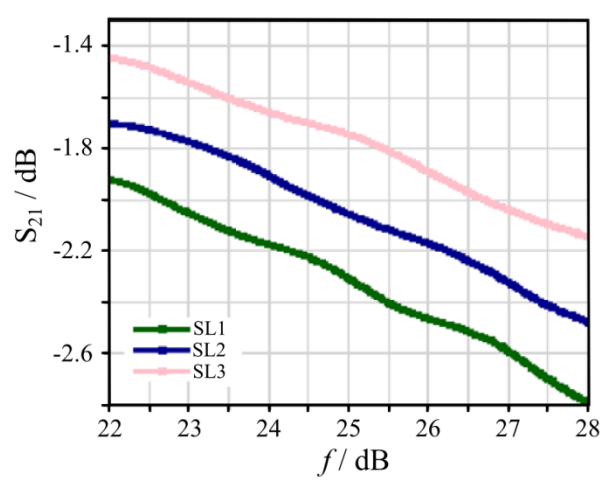

Figure 5: S_{21} parameter plotted as a function of frequency for the three microstrip lines SL1-3 on substrate SM2.

Table 2: Derived attenuation per unit length *a* of the 24 GHz microstrip lines for the different glass substrates and for the Rogers RO3003 substrate (R1).

Substrate	measured *g* / µm	targeted *g* / µm	*a* / dB/m
R1	79	76	78
AF32_1	78	76	83
AF32_2	75	76	238
AF32_3	86	76	143
AF32_4	76	76	116
AF32_8	73	76	118
AF32_9	70	76	106
AF32_10	70	76	109

is calculated from the S-parameters. It corrects the transmission by the reflection terms. In an ideal world it should give three straight lines, which are equidistant, as a function of frequency for the three different lengths of the microstrip lines. The data are fitted to a linear relationship, and the difference gives the loss of the microstrip line. In Table 2, we summarize the derived attenuation per unit length *a* for seven different glass substrates which use five different methods for metallization and structuring and compare it to corresponding structures on a 125 µm thick copper laminated RO3003 (R1). The attenuation which we obtain is roughly a factor of three larger than the attenuation reported by Rogers [2]. In [2], a value of 0.7 dB/inch = 27 dB/m is reported for laminate without any climate stress, whereas we measure a loss of 78 dB/m. This discrepancy might be a hint for non-perfect structures but it contradicts to our excellent match of the 50 Ω impedance. The attenuation of the structured glasses ranges between 83 dB/m and 238 dB/m which means that the details of the metallization and structuring processes differ a lot in high frequency performance. This also means that optimization of the metallization is crucial for high frequency performance. The solution of AF32_1 is an excellent compromise since in this case the glass is coated on both sides with a thin (15 µm) polymer layer of low-loss dry film dielectrics (Ajinomoto ABF GY11 with $\varepsilon = 3.2$, $\tan\delta = 0.0042$ at 5.8 GHz). Besides low dielectric loss it also shows good metal adhesion. From the structures where the metal was directly coated on the glass the substrates AF32_4 and AF32_8-10 show the best results. AF32_8-10 are metallized using the same process and demonstrate the reproducibility of the results.

As a next step the S-parameters for the 24 GHz ring resonators are measured. In this case a direct quantitative measure of the substrate quality is more difficult since the loaded *Q*-factor of the ring resonator depends on the dielectric losses, the metallization losses and the attenuation due to the vicinity of the microstrip line. A basic understanding of the last point is obtained by structuring always a pair of ring resonators with two different gaps (see Figure 2). Typically rs = 12 µm and rs = 48 µm, were targeted for structuring. In Figure 6 and Figure 7 we show representative S-parameters for the 24 GHz ring resonator structures. The Eigenresonance at 24.5 GHz can be clearly

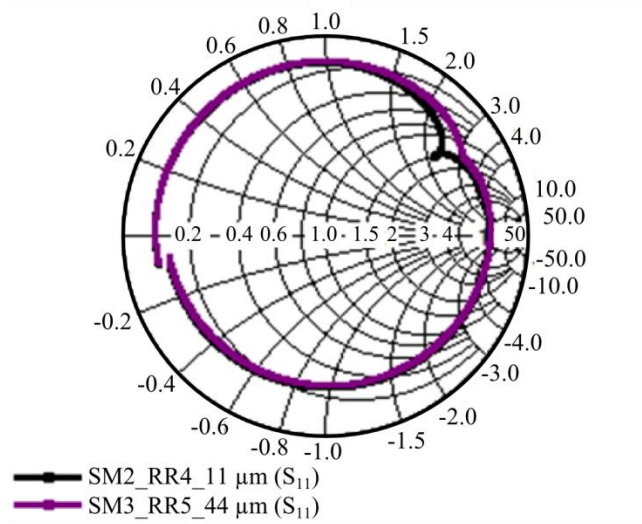

Figure 6: S-parameter S_{11} of the ring resonators RR4 and RR5 on substrate SM2=AF32_9 and SM3=AF32_10 with a slit width rs = 11 µm and rs = 44 µm, respectively.

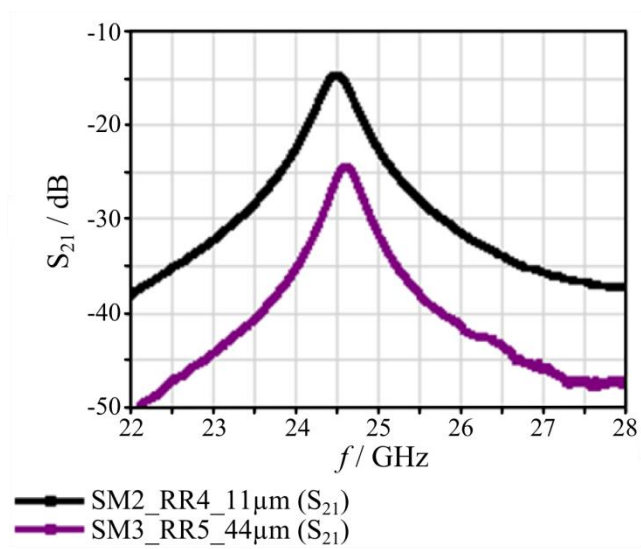

Figure 7: S-parameter S_{21} of the two ring resonators RR4 and RR5. It can be clearly seen that the smaller slit with rs = 11 µm allows to couple more energy into the ring resonator whereas the wider slit with rs = 44 µm allows to couple less energy into the resonator but improves the overall loaded quality factor *Q* of the resonator.

observed. The damping of the resonator and the energy which is coupled into the resonator differs strongly, depending on the width of the slit rs. The loaded quality factor *Q* of each ring resonator is obtained by fitting the S_{21} parameter to a Lorentzian line shape

$$S_{21}(\omega) = \frac{a}{((\omega-\omega_0+\frac{\omega_0}{8Q^2})^2+(\frac{\omega_0}{2Q})^2)} \quad (2)$$

Table 3: Slit width rs and obtained loaded Q-factor of the 24 GHz ring resonators are shown. The Q-factors are only slightly larger than the ones of the RO3003 substrate (R1).

Substrate – No. of Ring Resonator	measured rs / µm	targeted rs / µm	Q
R1 – RR 4	56	19	73
R1 – RR 5	58	6	73
AF32_1 – RR 4	50	19	58
AF32_1 – RR 5	50	19	59
AF32_1 – RR 5a	5	6	44
AF32_2 – RR 5	46	48	61
AF32_3 – RR 5	95	48	68
AF32_4 – RR 4	35	12	65
AF32_5 – RR 5	69	48	68
AF32_8 – RR4	11	12	56
AF32_8 – RR5	48	48	65
AF32_9 – RR4	11	12	56
AF32_9 – RR5	44	48	66
AF32_10 – RR4	10	12	56
AF32_10 – RR5	44	48	66

with an Eigenresonance ω_0 and a quality factor Q. The results for the obtained ring resonators are shown in Table 3. As an overall result of the 24 GHz structure we conclude that it is possible to make 24 GHz resonating and transmitting structures with good quality on glass. However the metallization process has to be chosen carefully.

IV. Measurement at 77 GHz and 100 GHz

A similar procedure was performed for the frequency dependent measurement in the frequency range between 65 GHz to 110 GHz. In this case the structures were smaller and the contacting was done using a pair of infinity w-band probe heads with 100 µm GSG pitch. Due to the larger frequencies a hollow waveguide was needed to connect the probe heads. To determine the loss of a microstrip line, lines were manufactured with lengths of 7.1 mm, 12.1 mm and 17.1 mm. As an example we show the S-parameter S_{11} and S_{21} of six lines in the frequency range between 70 GHz to 105 GHz in Figure 8 and Figure 9. In the frequency range between 75 GHz to 100 GHz, a straight line was fitted into the T_{eff} value (see Eq. (1)). From that, the loss of the microstrip lines in units of dB/m was determined. Unfortunately, structures on the Rogers substrate were not measurable but for some glass structures reliable and reproducible values for the dielectric loss of the microstrip line were obtained. The results for 77 GHz and 100 GHz are listed in Table 4. A loss of several hundred dB/m can clearly not be neglected but allows to integrate small structures in the frequency range up to 110 GHz on such a glass substrate.

Also ring resonators were processed on the substrates. For 77 GHz a ring resonator with an inner diameter of 1.05 mm and an outer diameter of 1.37 mm was structured.

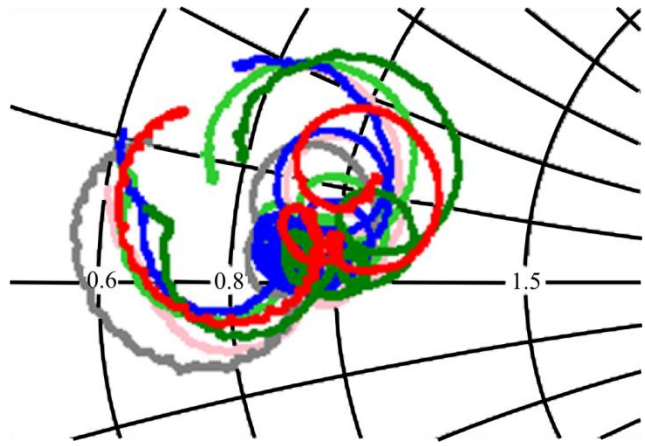

Figure 8: S_{11} parameter plotted in the complex plane (Smith chart) for the six microstrip lines S1-3 and S5-7 on substrate AF32_10.

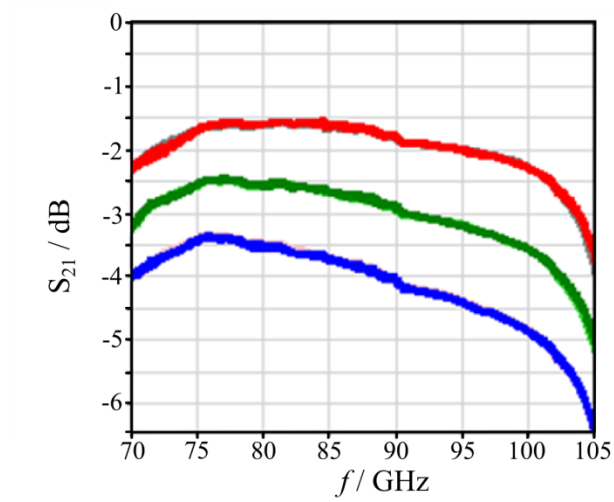

Figure 9: S_{21} parameter plotted as a function of frequency for the six microstrip lines S1-3 and S5-7 on substrate AF32_10.

The first harmonic of such a ring resonates at 77 GHz according to field simulation investigations using CST studio.

The results of the 77 GHz ring resonators are summarized in Table 5. Depending on the details of the metallization and structuring process and depending on the width of the gap on the ring (see Figure 2) loaded Q-values of up to $Q = 54$ were obtained. The substrates AF32_5-7 and AF328-10 are each metallized with identical processes and demonstrate the reproducibility of the results.

The 100 GHz resonating structures were designed in a little different way. The rings were made with an inner diameter of 1.4 mm and an outer diameter of 1.56 mm. In this way they show a resonance in the first harmonic around 69 GHz and for the second harmonic around 100 GHz. The results are shown in Table 6.

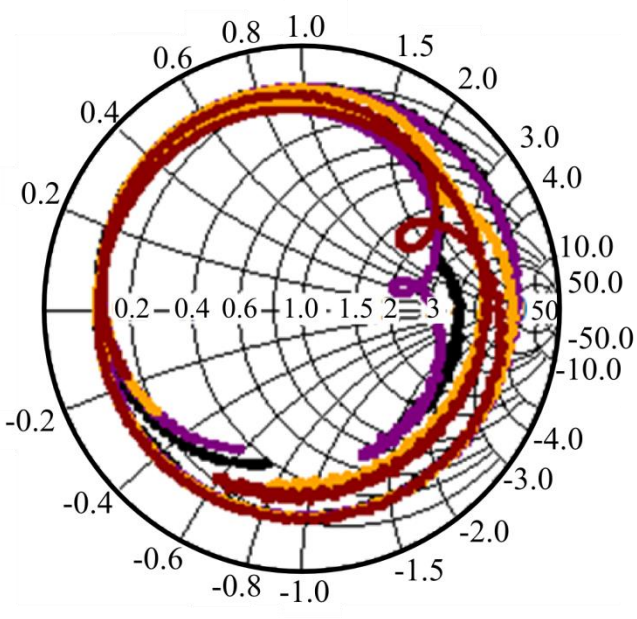

Figure 10: S_{11} parameter plotted in the complex plane (Smith chart) in the range between 65 GHz and 110 GHz for the four ring resonators RR4,5,8 and 9 on substrate AF32_10.

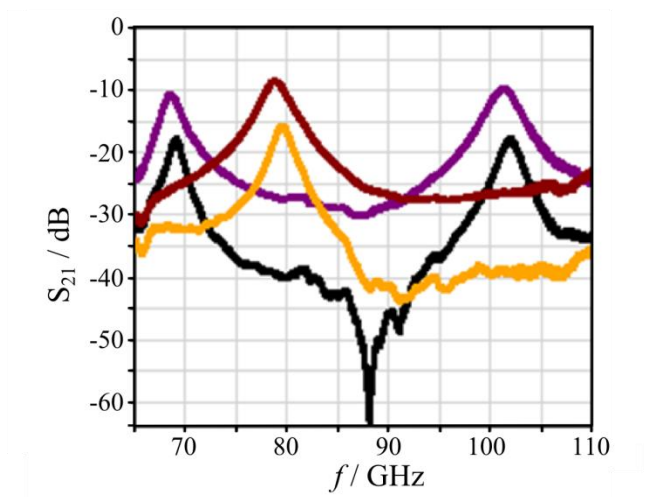

Figure 11: S_{12} parameter plotted as a function of frequency for the four ring resonators RR4,5,8 and 9 on substrate SM3. The 77 GHz resonance with the two different couplings to the ring resonator can be clearly observed as well as the two resonances around 69 GHz and around 100 GHz of the 100 GHz structures.

Table 4: Attenuation *a* of the microstrip lines of identical glass substrates with different metallization procedures. The realized and targeted slit width *g* of the GSG coplanar contact pads are given.

Substrate	measured *g* / µm	targeted *g* / µm	77 GHz *a* / dB/m	100 GHz *a* / dB/m
AF32_1	17	20	309	420
AF32_1	17	20	318	477
AF32_2	12	20	391	549
AF32_5	33	20	359	519
AF32_5	33	20	354	500
AF32_6	53	20	386	504
AF32_6	53	20	335	483
AF32_7	39	20	353	511
AF32_8	24	20	359	502
AF32_9	22	20	356	512
AF32_10	24	20	360	513

Table 5: Properties of the ring resonators around 77 GHz

Substrate – No. of Ring Resonator	measured rs / µm	targeted rs / µm	*Q*
AF32_1 – RR 9	4	19	26
AF32_2 – RR 10	49	40	53
AF32_5 – RR 10	64	40	43
AF32_5 – RR 4	49	10	48
AF32_5 – RR 5	67	40	54
AF32_5 – RR 9	47	10	47
AF32_6 – RR 10	78	40	35
AF32_6 – RR 4	63	10	49
AF32_6 – RR 5	84	40	50
AF32_6 – RR 9	61	10	52
AF32_7 – RR8	43	40	43
AF32_7 – RR9	39	10	53
AF32_7 – RR4	51	10	48
AF32_7 – RR5	68	40	51
AF32_8 – RR8	40	40	41
AF32_8 – RR9	13	10	29
AF32_9 – RR8	43	40	42
AF32_9 – RR9	15	10	28
AF32_10 – RR8	43	40	43
AF32_10 – RR9	13	10	30

Table 6: Properties of the ring resonators around 100 GHz

Substrate – No. of Ring Resonator	measured rs / µm	targeted rs / µm	*Q*
AF32_1 – RR 9	4	19	24
AF32_2 – RR 10	49	40	52
AF32_5 – RR 10	64	40	57
AF32_5 – RR 9	47	10	53
AF32_6 – RR 10	78	40	53
AF32_6 – RR 9	61	10	56
AF32_7 – RR 9	39	10	53
AF32_7 – RR 10	65	40	56
AF32_8 – R4	36	40	49
AF32_8 – R5	7	10	32
AF32_9 – R4	45	40	50
AF32_9 – R5	19	10	34
AF32_10 – R4	44	40	49
AF32_10 – R5	14	10	34

Table 1. Properties of the ring resonators around 100 GHz.

V. CONCLUSION

In summary we have shown that efficient structures with reasonable small dielectric loss at frequencies between 24 GHz and 100 GHz can be built using 100 µm thin SCHOTT glass AF32_eco as a substrate material. Also resonating structures which show resonances at 24 GHz, at 77 GHz and at 100 GHz in combination with reasonable *Q*-factors were demonstrated. A careful optimization and a careful choice of the metallization process and of the structuring method are needed. Larger data rates also contain higher frequency components and become important for e.g. interposers and high power computing. Using glass as a substrate, can make use of the results presented in the current work.

ACKNOWLEDGMENTS

We acknowledge support from the IAB program of the PRC. We thank Rolf Jakoby from the TU Darmstadt for his support of this project.

REFERENCES

[1] M. Letz, M. Jotz, R. Sprengard, „Glass: a universal material class for semi-conductor packaging and further integration“, Chip Scale Review, 21(3), 37 (2017)

[2] Rogers product information, MVP “New laminates enable 79 GHz Technology Advancements”, Microwave Journal 58(12) 2015

[3] C. S. Lam, "A review of the timing and filtering technologies in smartphones," 2016 IEEE International Frequency Control Symposium (IFCS), New Orleans, LA, 2016, pp. 1-6. doi: 10.1109/FCS.2016.7546724

[4] Y. H. Chen et al., "20" x 20" Panel Size Glass IPD Interposer Manufacturing," 2016 IEEE 66th Electronic Components and Technology Conference (ECTC), Las Vegas, NV, 2016, pp. 2146-2150. doi: 10.1109/ECTC.2016.400

[5] M.Letz et al. “Glass in Electronic Packaging and Integration: High Q Inductances for 2.35 GHz Impedance Matching in 0.05 mm Thin Glass Substrates” 2018 IEEE 68th Electronic Components and Technology Conference DOI: 10.1109/ECTC.2018.00167

[6] S. Onitake and T. Onishi, "Direct copper metallization on glass technology + x-substrate," 2017 IMAPS Nordic Conference on Microelectronics Packaging (NordPac), Gothenburg, 2017, pp. 35-37. doi: 10.1109/NORDPAC.2017.7993159S.

[7] Z. Wu, J. Min, V. Smet, M. R. Pulugurtha, V. Sundaram, R. R. Tummala, “Ultra-miniaturized 3D IPAC Packages with 100 µm Thick Glass Substrates for RF Front-end Modules”, *Journal of Electronic Packaging*, 2017, Vol. 13, No. 3, pp. 041001.

[8] J. Hasch, E. Topak, R. Schnabel, T. Zwick, R. Weigel and C. Waldschmidt, "Millimeter-Wave Technology for Automotive Radar Sensors in the 77 GHz Frequency Band," in IEEE Transactions on Microwave Theory and Techniques, vol. 60, no. 3, pp. 845-860, March 2012.

[9] R. Tummala, “Moore’s law for packaging to replace Moore’s law for IC’s”, Chip Scale Review, 23(1), 31 (2019)

[10] A. Shorey et al., “Addressing Next Generation Packaging and IoT with Glass Solutions”, IMAPS Additional Conferences (Device Packaging, HiTEC, HiTEN, & CICMT), DPC, 1-19 (2017)

[11] A. O. Watanabe et al., "First Demonstration of 28 GHz and 39 GHz Transmission Lines and Antennas on Glass Substrates for 5G Modules," 2017 IEEE 67th Electronic Components and Technology Conference (ECTC), Orlando, FL, 2017, pp. 236-241.

[12] Z. Wu, J. Min, M. S. Kim, M. R. Pulugurtha, V. Sundaram, R. R. Tummala, “Design and Demonstration of Ultra-thin Glass 3D IPD Diplexers”, in *2016 Proceedings 66th ECTC*, pp. 2348-2352, Las Vegas, NV, 2016.

[13] Jun-Bo Yoon, Bon-Kee Kim, Chul-Hi Han, Euisik Yoon, Kwyro Lee and Choong-Ki Kim, "High-performance electroplated solenoid-type integrated inductor (SI/sup 2/) for RF applications using simple 3D surface micromachining technology," International Electron Devices Meeting 1998. Technical Digest (Cat. No.98CH36217), San Francisco, CA, USA, 1998, pp. 544-547. doi: 10.1109/IEDM.1998.74641